Orientational Opacity Functions for the CN(A) and CN(B) Radical Formations in the $Ar(^3P)+CF_3CN$ Reaction

Dock-Chil CHE,# Toshio KASAI,* Hiroshi OHOYAMA, and Keiji KUWATA
Department of Chemistry, Faculty of Science, Osaka University, Toyonaka, Osaka 560
(Received December 17, 1993)

Using the oriented molecular beam, the orientational dependence of the CN(A) and of the CN(B) radical formation has been reinvestigated to obtain orientational opacity functions for the $Ar(^3P)+CF_3CN$ reaction. The steric model with the Legendre polynomial expansion gave the best-fit functions which have two reactive sites on CF_3CN. One site locates at the CN end and the other one near the C–F bonds. It was found that the CF_3 end attack is the least favorable for both CN formations. These results substantiate the relationship between the shape of the 2e and $7a_1$ molecular orbitals of CF_3CN and the orientational opacity functions.

Over the years, theories and experiments have shown the importance of mutual orientation of reactant molecules for rate, branching, and pathways of reaction.[1—7] The orientational opacity functions for an elementary reaction afford directly a quantitative information about steric effects. Through analysis of opacity function, we will be able to understand how reaction occurs and how effectively they are controlled.

Deexicitation reactions of metastable atoms with molecules are prototypical reactions for energy transfer.[8—12] As a sequel of the studies on the energy transfer reactions such as CX_3Y (X=H, D, and F; Y=CN and H),[13—15] we recently investigated effects of molecular orientation in the $Ar(^3P)+CF_3CN$ reaction.[16,17] The analysis with the painted hard-sphere model showed that the CN end attack by Ar (^3P), or Ar*, was more favorable than the CF_3 end attack for producing the excited CN radicals in the A and B states. The stereo anisotropy, i. e. the ratio of the reaction probability for the CN end attack to that for the CF_3 end attack, was found to be 1.5 and 1.6 for the CN(A) and the CN(B) radical formation, respectively.[17] These steric effects were qualitatively explained in terms of the shapes of the HOMO and HOMO-1 molecular orbitals of CF_3CN. The similarity in steric effect for the two CN formations suggested the presence of a common excited state, such as the Rydberg state/states of CF_3CN. The photodissociation of CF_3CN in the vacuum ultraviolet region has also suggested the 3s Rydberg state of CF_3CN as the excited state.[18,19]

Since orientational opacity function is a general expression for steric effects, we reinvestigated orientational dependence of the CN radical formation by measuring the stereo anisotropy as a function of the hexapole rod voltage.[4,5] The results in the present study are compared with those in the painted hard-sphere model. The relationship between the shape of the orientational opacity function and the spatial distributions of the $7a_1$ and the 2e orbitals, and the electron exchange mechanism are examined.

#Present address: Department of Chemistry, Rice University, P. O. Box 1892, Houston, TX 77251 USA.

Experimental

CF_3CN is a symmetric top molecule which can be oriented prior to reaction by electric hexapole field. Molecules with "right" orientations, i.e. molecules with the positive $<\cos\theta>$ $(=KM/(J^2+J))$ by definition, can pass through the hexapole field, and molecules with "wrong" orientations, or the negative $<\cos\theta>$ are filtered out by the same field. Here, θ is the angle between the molecular axis and the direction of the electric field, and J, K, and M are rotational quantum numbers for a symmetric top.[22] Such rotational state-selected molecules in a beam cross a beam of Ar* in a reaction chamber. The crossed beam zone is set within a uniform field which makes the reagent molecules oriented with respect to the direction of the incoming Ar* atom. The uniform field prepares molecular orientation, one for the CF_3 end attack and another one for the CN end attack. The random orientation is prepared by grounding the uniform field. The violet emission, CN(B→X) and the red emission, CN(A→X) are measured by a photon count detector unit in the third direction under three collisional geometry conditions. The hexapole rod voltage, V_0 is varied to change the orientational distributions of the reagent CF_3CN. The crossed beam signals were averaged over 7500—36000 beam-pulses until the experimental error reaches to <5%. Table 1 lists the experimental conditions. The details of the apparatus and the experimental procedure are given elsewhere.[15,17]

The degree of orientation of the state-selected CF_3CN beam can be varied by varying the hexapole rod voltage, V_0 and the Monte Carlo trajectory calculations estimate the orientational distributions at various V_0.[23—25]

Table 2 lists the lowest eight Legendre moments for five hexapole voltages used in this study. The first term, C_1, corresponds to the degree of orientation and it becomes larger as V_0 increases, showing a better orientation at the low V_0.[23—25]

Figure 1 shows the calculated $W(\boldsymbol{r}\cdot\boldsymbol{E})$ of the CF_3CN beam at 0, 6, and 12 kV after the hexapole state-selection, and the polar coordinate representation of $W(\boldsymbol{r}\cdot\boldsymbol{E})$ is presented in the inner panel.[17] The distribution marked as "random" represents the orientational distribution for the unoriented molecules. Molecules in a specific rotational state tend to loose their quantization axis in the absence of the electric field. So the random orientation is prepared by grounding the uniform field. Since $W(\boldsymbol{r}\cdot\boldsymbol{E})$ is the superposition of individual rotational wavefunctions of the molecule,

Table 1. Experimental Conditions for the Reagent Beams

	Stagnation pressure	Stream velocity	Translational temperature
	Torr[a)]	$m\,s^{-1}$	K
CF_3CN	60	435±10	61±5
$Ar(^3P)$	125	650±10	45±5

a) 1 Torr=133.322 Pa.

Table 2. Legendre Moments of the Orientational Distributions for the CF_3CN Beam after the Hexapole Field State-Selection at Various V_0

	Hexapole rod voltage/kV				
	6.0	7.0	8.0	10.0	12.0
C_1	0.623	0.607	0.591	0.555	0.520
C_2	0.219	0.196	0.174	0.128	0.086
C_3	0.026	0.013	0.002	−0.019	−0.031
C_4	−0.005	−0.008	−0.010	−0.009	−0.002
C_5	0.003	0.003	0.002	0.005	0.008
C_6	0.003	0.004	0.002	0.002	0.000
C_7	−0.001	0.001	0.000	0.000	−0.002
C_8	−0.001	−0.001	−0.001	−0.001	−0.001

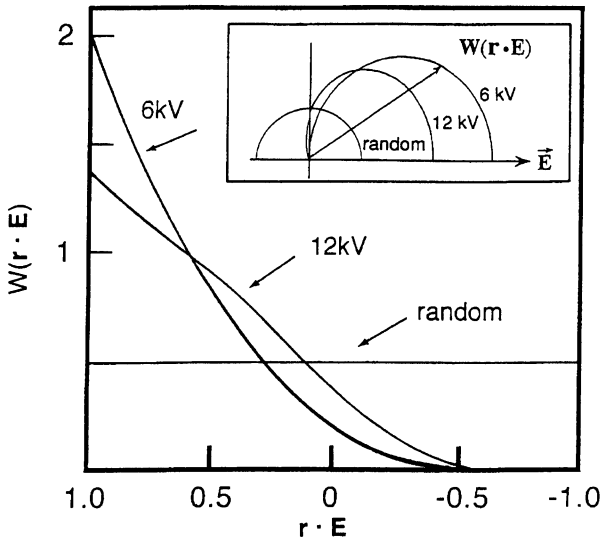

Fig. 1. Calculated orientational distributions $W(\boldsymbol{r}\cdot\boldsymbol{E})$, $\boldsymbol{r}\cdot\boldsymbol{E}=\cos\theta$, of the CF_3CN beam after the hexapole field at 0 kV (indicated as "random"), 6, and 12 kV. The inner panel shows the polar coordinate representation of those distributions.

it may penetrate into the opposite (or negative) region of the orientational angle, like we see the $W(\boldsymbol{r}\cdot\boldsymbol{E})$ of 6 and 12 kV in the figure. In order to recall the fact that $W(\boldsymbol{r}\cdot\boldsymbol{E})$ is V_0-dependent, it may be rewritten as $W_{V_0}(\cos\theta)$, where $\boldsymbol{r}\cdot\boldsymbol{E}$ is replaced by $\cos\theta$.[4,5,26)]

$$I(V_0) = I(V_0;\text{on})/I(V_0;\text{off}). \quad (1)$$

The orientational opacity function can be obtained from the normalized emission intensities, $I(V_0)$ for the CF_3 end and for the CN end orientation at various V_0. Such $I(V_0)$ is expressed by the division of the emission intensity with active uniform field, $I(V_0;\text{on})$, by the emission intensity with null field, $I(V_0;\text{off})$, as shown in Eq. 1.[7)] So that $I(V_0;\text{on})$ gives a signal from the oriented molecules, and $I(V_0;\text{off})$ gives a reference signal from the same number of molecules but with "random" orientation. Thus after the normalization, $I(V_0)$ merely reflects the steric effect, or the stereo anisotropy in reaction.

$$I(V_0) = \int_{-1}^{1} I(\cos\gamma)W_{V_0}(\cos\gamma)\mathrm{d}\cos\gamma. \quad (2)$$

Equation 2 expresses how to link $I(V_0)$ to the opacity function, $I(\cos\gamma)$, using the orientational distribution, $W_{V_0}(\cos\gamma)$. Here the orientational angle, θ, is replaced by γ for stressing the meaning of the angle as the attacking angle in the opacity function.

$$I(\cos\gamma) = \sum_n S_n P_n(\cos\gamma). \quad (3)$$

Since $I(\cos\gamma)$ has the symmetry, by definition, with respect to the azimuthal angle of the molecule, it can be expanded by Legendre polynomials, $P_n(\cos\gamma)$ as shown in Eq. 3, where S_n is coefficients of Legendre polynomials, and γ is the angle between the molecular axis and the direction of the incoming Ar^*.[4,5,26)] The best-fit procedure of $I(\cos\gamma)$ by finding the most probable S_n for the $I(V_0)$ and $W_{V_0}(\cos\gamma)$ experimentally obtained enables us to find out the most probable opacity function.

Results

Figure 2 shows the V_0-dependence of $I(V_0)$ for the CN(B→X) emission with the open circles and for the CN(A→X) emission with the filled circles. Since $I(V_0)$ is the normalized emission, it is decoupled from any other systematic changes like the beam intensity, and it is solely due to the effect of molecular orientation. Because of this, the absolute values of the $I(V_0)$ for either molecular orientation increase with the decrease of V_0. For the degree of orientation becomes better with the decrease of V_0.

The best-fit simulated curves for the $I(V_0)$ of the CN(B→X) emission give a set of S_n as shown in Table 3. Similarly, the S_n for the CN(A→X) emission are listed in Table 4. Those Legendre expansion coefficients synthesize the most probable $I(\cos\gamma)$. It was found that the third-order Legendre expansion (i.e. $n=0$—3) fits the $I(V_0)$ best with the given experimental inaccuracy in either case of the radical formation. The orientational opacity functions for the CN(B) and the CN(A) formations thus obtained are shown in Fig. 3.[15)]

Both functions show a close resemblance in shape and there are two peaks which correspond to two reactive sites on the molecule. One site locates at the C–N bond

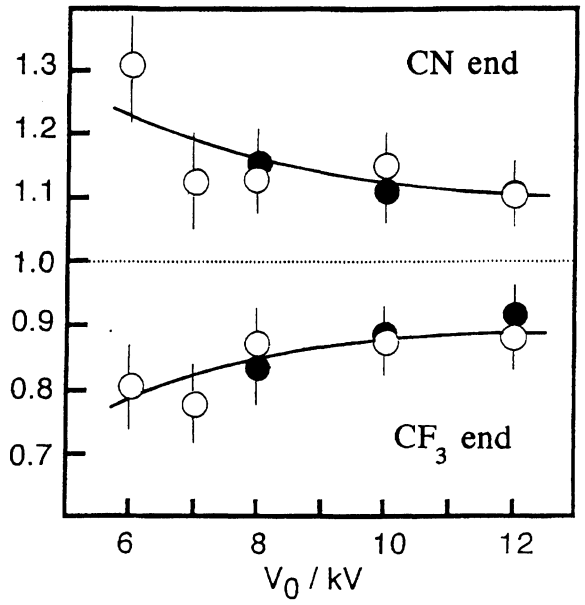

Fig. 2. V_0-dependence of the normalized emission intensities of CN(B→X) with the open circles and of CN(A→X) with the filled circles for the CN end (the upper data points) and the CF_3 end orientation (the lower data points), respectively. The experimental uncertainty is indicated with the bars. The solid curves were obtained by the Legndre best-fit.

Table 3. Legendre Expansion Coefficients of the $I(\cos\gamma)$ for the CN(B→X) Emission

	The highest term of the expantion, N		
	1	2	3
S_0[a)]	1.00	1.00	1.00
S_1	0.27	0.27	0.28
S_2		0.01	0.01
S_3			1.14

a) The S_0 is set as 1.00 to meet the measurement condition for the normalized emission intensity.

Table 4. Legendre Expansion Coefficients of the $I(\cos\gamma)$ for the CN(A→X) Emission

	The highest term of the expantion, N		
	1	2	3
S_0[a)]	1.00	1.00	1.00
S_1	0.22	0.22	0.26
S_2		0.03	0.04
S_3			1.21

a) The S_0 is set as 1.00 to meet the measurement condition for the normalized emission intensity.

area at $\cos\gamma=1.0$ and another near $\cos\gamma\approx-0.5$, but there is the least reactive area at the CF_3 end, $\cos\gamma=-1.0$.

Discussion

Figure 4 shows the polar coordinate representation

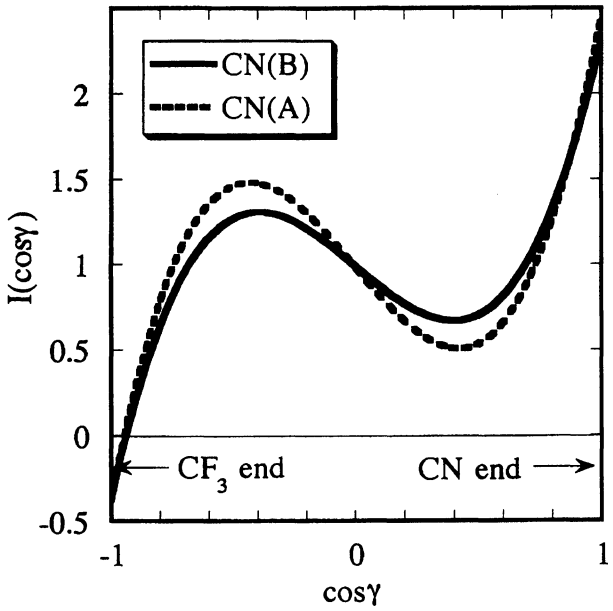

Fig. 3. Orientational opacity functions, $I(\cos\gamma)$, for the radical formations of CN(B) (the solid line) and CN(A) (the broken line). Both functions show two reactive sites; one locates at the CN end ($\cos\gamma=1.0$) and the other is located near $\cos\gamma\approx-0.5$.

of the opacity function for the CN(B) formation. The orientational opacity function for the CN(A) formation (the broken line in Fig. 3) was found to be nearly the same, so we only show the one as representative. The van der Waals surface of the CF_3CN molecule is also shown with the broken line just for reference, which is regarded to be a measure of the electron density distribution of the outer shell orbitals.[27] The earlier studies on the reaction of Ar* with CH_3CN or CD_3CN showed that the orientation-dependence for the CN(B) formation was explained in relation to the spatial distribution of the anisotropic $7a_1$ and of the isotropic 2e molecular orbitals, assuming that the electron exchange mechanism is a dominant process for the energy transfer.[13,14]

In the electron exchange mechanism, an outer shell

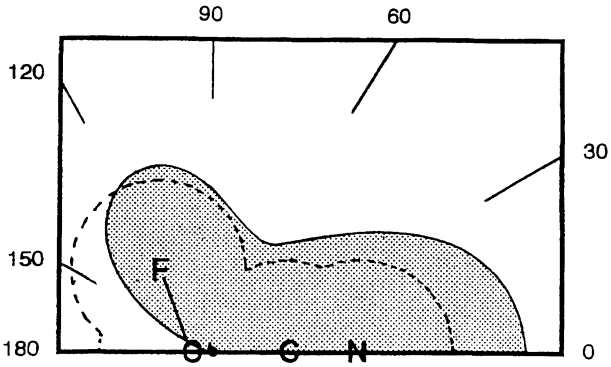

Fig. 4. Polar coordinate representation of the orientational opacity function for the CN(B) formation. The van der Waals surface of the CF_3CN molecule is shown with the broken line.

electron of a molecular orbital, MO, is ejected to the vacant 3p orbital of Ar^*, and simultaneously the 4s electron of Ar^* moves to a Rydberg orbital of the molecule, Ryd. The probability of such electron exchange is proportional to the square of the exchange matrix as shown in Eq. 4.[21,28,29]

$$P(R,\gamma) \propto |< 3p(1)Ryd(2) \mid 1/r_{12} \mid MO(1)4s(2) >|^2, \quad (4)$$

where R is the distance between the reactant molecule and the atom, and γ is the orientational angle, while r_{12} is the distance between exchanging two electrons. The exchange probability thus becomes an explicit function of the molecular orientation γ. As the equation shows, the initial electronic state is expressed by the product of the 4s atomic orbital and the molecular orbital MO. Similarly, the final electronic state is expressed by the product of the molecular Rydberg orbital MO and the 3p atomic orbital. Since the electronic wavefunctions of the atom and the molecule must overlap efficiently for the electron exchange, the probability of the exchange is expected to be orientational dependent. Because of the bulkiness of the 4s orbital and of the Rydberg orbital, the overlap of the MO and the 3p orbitals could become significant. As a consequence, the spatial distribution of the MO tends to be responsible to the γ-dependence of the exchange probability, thus it reaches the close connection between the spatial distribution of MO and the shape of the opacity function.[15,21]

The VUV-photoexcitation studies suggested that the $7a_1$ and 2e molecular orbitals of CF_3CN play a key role in the CN formations.[18,19] The $7a_1$ orbital has a character of non-bonding and it locates at the CN end of the molecule. The 2e orbital locates around the C–F bonds and also on the C–N bond. It is known that these two orbitals have nearly the same energy and the excitation spectra for the CN(A) and CN(B) gave the same pattern in shape in the photoexcitation of CF_3CN.[18,19] It is therefore worthwhile recalling again that the orientational opacity functions for the CN(B) and CN(A), obtained in the present study, are found to be similar in shape to the spatial distributions of the $7a_1$ and 2e orbitals. This similarity qualitatively justifies the assertion that the electron exchange mechanism is the major energy transfer process in this reaction. Theoretical calculations are necessary to confirm the mechanism quantitatively in the future studies.

This work was partially supported by a Grant-in-Aid for Scientific Research No. 2191 from the Ministry of Education, Science and Culture.

References

1) P. R. Brooks, *Science*, **193**, 11 (1976).
2) S. Stolte, *Ber. Bunsen-Ges. Phys. Chem.*, **86**, 413 (1982).
3) R. B. Bernstein, D. R. Herschbach, and R. D. Levine, *J. Phys. Chem.*, **91**, 5365 (1987).
4) S. Stolte, "Atomic and Molecular Beam Method," ed by G. Scoles, Oxford Univ. Press, New York (1988), Vol. 1, p. 631.
5) D. H. Parker and R. B. Bernstein, *Annu. Rev. Phys. Chem.*, **40**, 561 (1989).
6) P. W. Harland, H. S. Carman, Jr., L. F. Phillips, and P. R. Brooks, *J. Phys. Chem.*, **95**, 8137 (1991).
7) T. Kasai, T. Matsunami, T. Fukawa, H. Ohoyama, and K. Kuwata, *Phys. Rev. Lett.*, **70**, 3864 (1993).
8) D. H. Stedman, and D. W. Setser, *Prog. React. Kinet.*, **6**, 4 (1971).
9) J. A. Coxon, D. W Setser, and W. H. Duwer, *J. Chem. Phys.*, **58**, 2244 (1973).
10) J. E. Velazco, J. H. Kolts, and D. W. Setser, *J. Chem. Phys.*, **69**, 4357 (1978).
11) J. Balamuta, M. F. Golde, and Y-S. Ho, *J. Chem. Phys.*, **79**, 2822 (1983).
12) T. Nagata, K. Kondow, K. Kuchitsu, S Tabayashi, S. Ohshima, and K. Shobatake, *J. Phys. Chem.*, **89**, 2916 (1985).
13) T. Kasai, D.-C. Che, K. Ohashi, and K. Kuwata, *Chem. Phys. Lett.*, **163**, 246 (1989).
14) D.-C. Che, T. Kasai, H. Ohoyama, K. Ohashi, T. Fukawa, and K. Kuwata, *J. Phys. Chem.*, **95**, 8159 (1991).
15) H. Ohoyama, T. Kasai, K. Ohashi, and K. Kuwata, *Chem. Phys.*, **165**, 155 (1992).
16) D.-C. Che, T. Kasai, H. Ohoyama, and K. Kuwata, "15th International Symposium on Molecular Beams," Berlin, 1993, Abstr., No. H. 13. 1.
17) D.-C. Che, T. Kasai, H. Ohoyama, and K. Kuwata, *J. Phys. Chem.*, **1993**, in press.
18) M. N. R. Ashford and J. P. Simons, *J. Chem. Soc., Faraday Trans. 2*, **74**, 1263 (1978).
19) D. -C. Che, T. Kasai, H. Ohoyama, K. Kuwata, M. Kono, K. Tabayashi, and K. Shobatake, *Chem. Lett.* (1993), in press.
20) Y. Fukunishi, T. Kasai, and K. Kuwata, *Chem. Phys.*, **177**, 85 (1993).
21) H. Takahashi, H. Ohoyama, T. Kasai, K. Kuwata, M. Nakano, and K. Yamaguchi, submitted to *Chem. Phys. Lett.*, (1993).
22) C. H. Townes, and A. L. Schawlow, "Microwave Spectroscopy," McGraw-Hill, New York (1955).
23) K. K. Chakravorty, D. H. Parker, and R. B. Bernstein, *Chem. Phys.*, **68**, 1 (1982).
24) S. E. Choi and R. B. Bernstein, *J. Chem. Phys.*, **85**, 150 (1986).
25) T. Kasai, T. Fukawa, T. Matsunami, D.-C. Che, K. Ohashi, H. Ohoyama, and K. Kuwata, *Rev. Sci. Instrum.*, **64**, 1150 (1993).
26) S. Stolte, K. K. Chakravorty, R. B. Bernstein, and D. H. Parker, *Chem. Phys.*, **71**, 353 (1982).
27) K. Ohno, S. Matsumoto, K. Imai, and Y. Harada, *J. Chem. Phys.*, **93**, 206 (1984).
28) H. Hotop and A. Niehaus, *Z. Phys.*, **228**, 68 (1969).
29) W. H. Miller and H.Morgner, *J. Chem. Phys.*, **67**, 4923 (1977).